Acta Mechanica Slovaca **27 (2): 6 - 11,** June **2023**
https://doi.org/10.21496/ams.2022.018

Acta Mechanica Slovaca
ISSN 1335-2393
www.actamechanica.sk

Mathematical Model and Simulation of in-pipe Robot

Peter Ján Sinčák [1,*], Tomáš Merva [1], Ivan Virgala [1], Michal Kelemen [1]

[1] Technical University of Košice, Faculty of Mechanical Engineering, Letná 9, 04200 Košice, Slovak Republic

Abstract: At a time when most professions are undergoing massive automation and transformation there are still quite a few professions that have not changed in the past fifty years. One of those professions is chimney sweeping. This thought led to the initial idea for this paper. In this paper, we have proposed a design of an in-pipe robot that could be used for chimney cleaning and inspection. Mathematical modelling of the movement of the robot and actuators was carried out, which allowed us to study the proposed design. Since the mathematical model is quite abstract, computer simulations were done in order to prove the mathematical model, with the possibility to further parameters adjustment of the robot. After the simulations were concluded, the total distance and total time of one cycle of the actuator were obtained.

Keywords: mathematical modelling; simulation; robotics; in-pipe robot, inspection

1. Introduction

To prevent the build-up of highly flammable material such as soot in chimneys, the sweeping needs to be done regularly. The process of chimney sweeping consists of two main steps: cleaning and inspection. The cleaning part is executed by inserting a weighted chimney brush into the chimney and sliding it up and down thereafter. This is often performed at the height of tens of meters above the ground, which represents a safety hazard. The next part is a visual inspection that is usually done by only checking the chimney with a flashlight. The accuracy of the inspection depends solely on the experience and eyesight of a chimney sweeper.

We contend that chimney sweeping can be done more safely and accurately by having the in-pipe robot clean as well as inspect the chimney. The contribution of this paper is twofold. Firstly, we introduce the novel design of an in-pipe robot that is capable of doing both parts of the chimney sweeping process. Secondly, we provide a simulation model of the motion of the robot. The main feature of the robot is that it utilizes brushes for its movement, which results in performing the cleanup as well. Additionally, the modularity of the robot provides a user with the platform to interchange different kinds of brushes and devices necessary for chimney sweeping, such as a camera for inspection.

Most recent work in in-pipe robots can be categorized into two main groups: synthetic and biologically inspired. The movement strategy of the synthetic group is based on artificial motion that is not found in nature, such as wheels or tracks. The most common design is to uniformly distribute wheels, so the robot is pressed against the wall from each side. [1] However, the surface of the pipe is dirty and usually not smooth so the wheel can easily slip. [2][3] The better solution is to use tracks, whose adaptability can handle complex environments and therefore increase the stability of

*** Corresponding author:** Peter Ján Sinčák, ***E-mail address:*** *peter.jan.sincak@tuke.sk*

the robot. On the other hand, both of these designs need separate cleaning devices, which results in higher cost and complexity. [4] [5]

The strategy of the biologically inspired group is to mimic the movement of animals and insects. The Inchworm type utilizes bending and extending its body to move from one point to another, which is highly effective in polluted pipelines. [6] The travelling wave type takes advantage of the multiple segments body structure to create a travelling wave pattern. [7] The bristle type is strongly related to ours, which uses flexible components that are in contact with the walls of a pipe. [8]

2. Design of in-pipe robot

One of the objectives of our research is the investigation of novel means of locomotion of robots. The following concept of the robot is intended as an in-pipe robot, which is used for the inspection and cleaning of the chimney. The majority of the regular chimneys have a circular cross-section, therefore in-pipe robots seem a viable option when it comes to the movement inside them.

The proposed structure can be seen in Figure 1. It consists of two bristles that are attached to the main body of the robot. The two bristles are regular bristles that are used for chimney cleaning, and they are altered so they could be screwed onto the main body, which makes the robot modular, and if needed various other units with equipment like sensors, and cameras could be added. On the top bristle, a spherical-shaped cone is screwed on. This part is supposed to prevent the robot to get stuck in cases, where other appliances connect to the main chimney line and get stuck. The main body of the robot has a circular cross-section and is made of aluminium. The main reason for aluminium is its lightweight and non-ferromagnetic features so that the body does not interfere with the electromagnets that are used for locomotion. As said, the essential part of the locomotion unit is two electromagnets. These two electromagnets attract each other, where one is fixed, and the other one is moving together with the shaft. On the other end of the shaft is an adjustable spring, that pulls back the electromagnet after they are turned off. This spring moves the electromagnet in the direction of the movement of the robot and when the electromagnet collides with the centre piece that is connected with the robot's body, it creates the necessary energy for the movement up inside of the chimney. The energy created during this collision is not substantial enough to move the robot by a great distance. However, this process is very quick and can be done repeatedly to achieve sufficient movement of the robot.

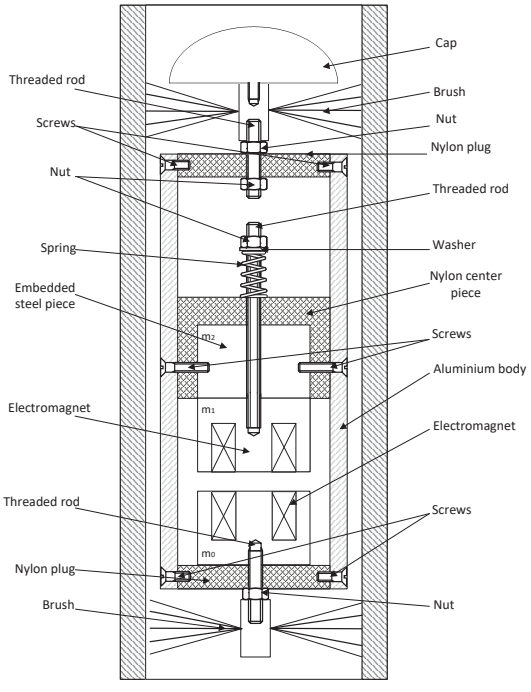

Figure 1: Schematic view of the proposed robot.

3. Mathematical model of robot's locomotion

The locomotion unit of this robot consists of two electromagnets that are opposite to each other. By turning on the electromagnets, one electromagnet is steady and the opposite one is able to move towards the steady electromagnet. As the electromagnet is moving, the spring is being pressed and energy is accumulated. When the electromagnets are subsequently turned off, the spring pulls back the moving electromagnet that collides with the steel centre piece that is connected to the main body of the robot. During this collision, the energy is generated and translated into the whole body of the robot. This energy is then the driving energy of the robot. To achieve the most efficient movement of the actuator and the whole robot, the movement is going to be described by mathematical equations. These movements are divided into four subsequent steps.

3.1. Step A

Step A is the initial point of the whole movement of the actuator. In this step, the electromagnets are turned on and the forces of attraction are attracting the moving electromagnet towards the steady electromagnet.

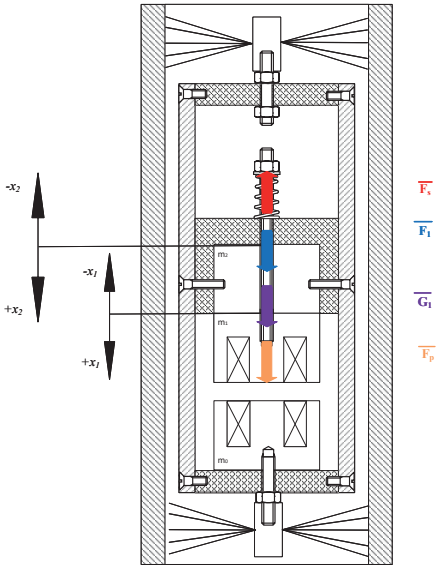

Figure 2: First step of the movement of the robot.

In figure 2, you can see vector forces that are acting in the step A. As you can see, F_p is the attraction force of the electromagnet and it is travelling in the positive direction of the coordinate system. G_1 is the gravitational force, which is affecting the moving electromagnet. F_1 is the friction force between the shaft, embed steel piece and nylon inside of the robot's body. F_S is the force caused by the pressing of the spring during the movement of the electromagnet. The label m_1 labelling the weight of the moving electromagnet and m_2 is the weight of the whole robot because the centrepiece is connected to the main body.

$$\frac{dx_1}{dt} = v_1(t) \tag{3.1}$$

$$\frac{dv_1}{dt} = \frac{1}{m_1}\left(F_p - F_1 - F_S + G_1\right) \tag{3.2}$$

$$\frac{dv_1}{dt} = \frac{1}{m_1}\left[F_p - F_1 - k.\left(x_1 - x_2\right) + m_1.g\right] \tag{3.3}$$

Equations (3.1), (3.2) and (3.3) describe a mathematical model of the forces that are acting in this movement. Previously mentioned equations were compiled on second Newton's law.

In equation (3.1), we defined that the change of the coordinate by the time is the velocity of the point that has changed its position. In the following equation (3.2) is applied second Newton's law to our case and it determines the relation between the forces and derivation of the velocity of the moving electromagnet by the time. In equation (3.3), we further developed an equation (3.2), where exactly F_S is equal to k, which is spring constant, multiplied by the change of the coordinates.

3.2. Step B

Step B is the second part of the movement of the actuator when the electromagnet reaches the other steady electromagnet and they are turned off. When they are turned off, the force that has accumulated in the spring is pulling the shaft with the electromagnet back to its initial position.

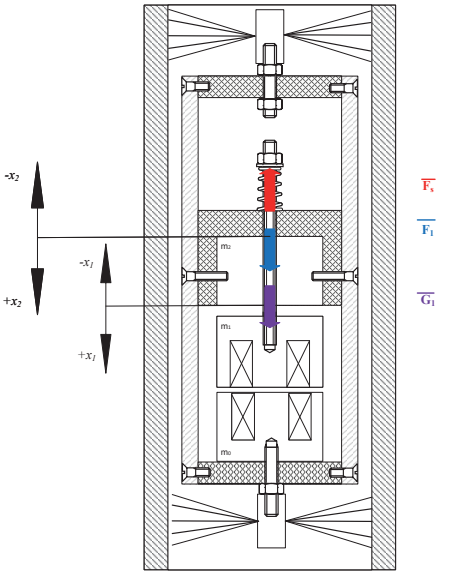

Figure 3: Second step of the movement of the robot.

As you can see in figure 3, the attraction force F_p has disappeared because the electromagnets are turned off. The friction force F_1 changed its direction, because the direction of the movement of the electromagnet has changed too. The rule of the opposite direction of the friction force against the direction of the movement was applied here.

$$\frac{dx_1}{dt} = v_1(t) \tag{3.4}$$

$$\frac{dv_1}{dt} = \frac{1}{m_1}\left(F_1 - F_S + G_1\right) \tag{3.5}$$

$$\frac{dv_1}{dt} = \frac{1}{m_1}\left[F_1 - k.(x_1 - x_2) + m_1.g\right] \quad (3.6)$$

In equation (3.5), you can see that the force F_p has disappeared and that the minus F_1 has changed to plus due to the opposite direction.

3.3. Step C

The third step in the movement of the actuator is when the moving electromagnet hits the initial surface and creates the driving force F_h.

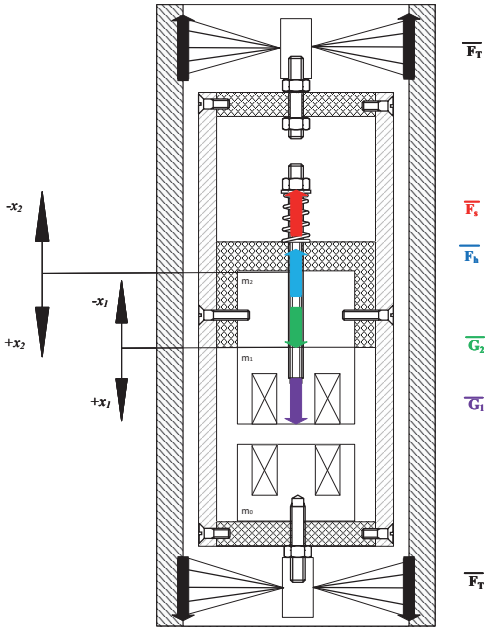

Figure 4: Third step of the movement of the robot.

In figure 4, you can see that the forces G_1 and F_S remained in the same direction as in the steps B and A. We also added a friction force F_T, which is friction force among brushes and the walls of the pipeline and driving force F_h that is caused by the hit. F_h equals to k_e which is the constant of the stiffness of the surface multiplied by the change of the coordinates. With the following equations (3.6), (3.7) and (3.8) we will model the situation when the electromagnet hits the surface.

$$\frac{dx_1}{dt} = v_1(t) \quad (3.7)$$

$$\frac{dv_1}{dt} = \frac{1}{m_1}\left(G_1 - F_S - F_h\right) \quad (3.8)$$

$$\frac{dv_1}{dt} = \frac{1}{m_1}\left[m_1.g - k(x_1 - x_2) - k_e(x_1 - x_2)\right] \quad (3.9)$$

The hit of the electromagnet caused the coordinates x_2 has changed, and therefore we had to compile the following equations with the condition $v_1 \geq 0$:

$$\frac{dx_2}{dt} = v_2(t) \quad (3.10)$$

$$\frac{dv_2}{dt} = \frac{1}{m_2}\left(-F_h + G_2 + F_T\right) \quad (3.11)$$

$$\frac{dv_2}{dt} = \frac{1}{m_2}\left[-k_e(x_1 - x_2) + F_T + m_2 g\right] \quad (3.12)$$

Equations (3.9), (3.10) and (3.11) are from the state of the weight m_2 just after the hit of the electromagnet when the change of the coordinates by the time was caused by the hit.

3.4. Step D

Step D in the motion of the actuator is the last motion. This last step represents the movement of the whole robot in the pipeline, which we compiled into the following equations:

$$\frac{dx_2}{dt} = v_2(t) \quad (3.13)$$

$$\frac{dv_2}{dt} = \frac{1}{m_2}\left[F_T(v_2) + G_2\right] \quad (3.14)$$

4. Simulation of mathematical model

The simulation of all four steps as one cycle was done in the programs MATLAB and Simulink. All four steps were modelled individually in Simulink, and a MATLAB script was used to connect the simulations, which can be seen in Algorithm 1. At the beginning of the Matlab code are all the parameters defined, that are used during the simulations. Weight m_1, which is the weight of a single electromagnet. Gravitational acceleration constant g. Spring constant k, which is determined by the type of the spring and was extracted from the spring catalogue given by the producer and the constant m_2, which represents the estimated total weight of the robot. The coefficient F_T represents the friction force among the brushes and the walls of the chimney and was chosen as the constant for the purpose of this simulation. Parameter k_e, which is called an equivalent stiffness coefficient, represents the deformation of the moving electromagnet and the steel piece during the collision. This parameter of the driving force F_h was obtained from the finite element method(FEM) simulation, where the electromagnet was on top of the steel piece and force F was acting

on the electromagnet. In equation (4.1) the relation between the equivalent stiffness coefficient, force and relative deformation can be seen.

$$k = \frac{F}{\Delta l} \tag{4.1}$$

$$y = kx + q \tag{4.2}$$

With this equation in mind and the equation of a straight line in equation (4.2), in FEM simulation the electromagnet was repeatedly loaded with different forces F and displacements were measured (Table 1.). The data in Table 1. are inserted in the graph and are forming a line, from there the coefficient k_e = 3E06 is extracted.

Table 1: Measured displacements during the FEM simulation

Force[N]	Displacement [mm]
0	0
5	1,70E-06
10	3,39E-06
15	5,09E-06
20	6,78E-06
25	8,48E-06
30	1,02E-05
35	1,19E-05
40	1,36E-05

The code in Algorithm 1 is graphically divided into four parts. Each part represents one of the phases that are being simulated in SIMULINK. In each of these parts, the simulation file is initialized, the simulation is being started, and the data from the simulations like the time of each step, velocity and travelled distance are stored in the workspace.

After all the simulations had run, the total time and total distance are calculated. The total distance that has been calculated is 1.0319 mm, and the total time is 0.0181 s. Both of these numbers are calculated with respect to the coefficients that were set at the beginning of the code. The total distance and total time are calculated in regard to one cycle of the actuator, which consists of steps A, B, C and D. Achieved total time and distance can be further improved by improving some of the variables and constants. With the help of the Matlab code, this can be done simply, just by trying different types of settings like changing the overall weight of the robot by making it from lighter material. Changing the coefficient k_e by hardening the embedded steel piece, since the electromagnet cannot be hardened, or by picking a different spring from the catalogue of the springs that are being produced, or by lowering the friction force between the brushes and walls of the chimney.

Algorithm1: Simulation of mathematical model in Matlab

1: Clear workspace
2: Initialization of variable and constants
3: ==========StepA==========
4: Start simulation of StepA
5: Save variables to the workspace
6: END the simulation of StepA
7:==========StepB==========
8: Start the simulation of StepB
9: Save variables to the workspace
10: END the simulation of StepB
11: ==========StepC==========
12: Start the simulation of StepC
13: Save the variables to the workspace
14: END the simulation of StepC
15: ==========StepD==========
16: Start the simulation of StepD
17: Save the variables to the workspace
18: END the simulation of StepD
19: Calculate the travelled distance of the robot
20: Calculate the total time t of one cycle

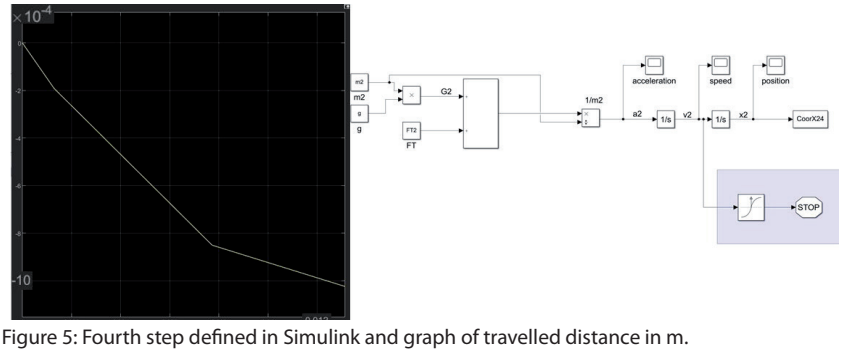

Figure 5: Fourth step defined in Simulink and graph of travelled distance in m.

5. Conclusions

One of the objectives of our research is the investigation of novel means of locomotion of robots. A novel design of an in-pipe/chimney cleaning robot has been introduced. This robot is using a new actuator that is based on creating a driving force during a collision. This actuator is composed of two electromagnets, that are attracting each other, where one is steady and the other one is moving. The moving electromagnet, during this movement, compresses a spring, which pulls back the electromagnet after they are turned off. After the electromagnet is pulled back, it collides with the centre steel piece that is connected to the body of the robot. During this collision, the driving force of the robot is created and the robot moves. This process represents one cycle of actuation. This cycle was mathematically described in chapter 3, where the cycle was divided into four steps. In chapter 4, the mathematical model was simulated using Matlab and Simulink. The script in Algorithm 1 represents the simulation of one cycle of the actuation. The result of this simulation was the total distance travelled by the robot, during one cycle, as well as the total time of this cycle. Even though the total distance travelled during this cycle is only 1.0319 mm the cycle time is 0.0181 s. This means that by quickly repeating this cycle the robot should theoretically be able to travel 50 mm in 1 s at the frequency of approximately 50 Hz of actuation. These results were achieved in the simulation, although the real-world application can differ from these numbers due to different conditions in chimneys or pipelines. The simulation can be used to further improve the performance of the robot by investigating the influence of the set parameters. For further research, we propose additional experimentation with the simulation model to achieve even greater travel distances of the robot during one cycle. After this, the application in real world should be tested to determine how does the sooth and dirt in the chimney influences the movement of the robot in real word. The area of robotic chimney cleaning is not well studied, however some advances in commercial chimney inspection were presented in [9-10]. Here the authors used drones, to fly inside a commercial chimney, that was carrying the camera or laser to perform the inspection of such chimneys. Other than that, the non-commercial robotic chimney inspection and cleaning is not well researched area and offers a great opportunity for further advancement and research.

Acknowledgements

This research was funded by Slovak Grant Agency VEGA 1/0436/22, VEGA 1/0201/21 and KEGA 030TUKE-4/2020.

References and Notes

1. Roh, S.; Kim, D.W., Lee, J.; Moon H.; Choi, H.R. In-pipe Robot Based on Selective Drive Mechanism. International Journal of Control, Automation, and Systems. 2009, 105-112. DOI: 10.1007/s12555-009-0113-z.
2. Deepak, B.B.V.L, Raju Bahubalendruni, M.V.A.; Biswal, M.V.A. Development of in-pipe robots for inspection and cleaning tasks. International Journal of Intelligent Unmanned Systems. 2016, 182-210.
3. Kakogawa, A.; Ma, S. Design of a multilink-articulated wheeled inspection robot for winding pipelines: AIRo-II. In Proceedings of the 2016 IEEE/RSJ International Conference on Intelligent Robots and Systems (IROS), Daejeon, Korea, 9–14 October 2016; pp. 2115–2121.
4. Nayak, A.; Pradhan, S. K. Design of a New In-Pipe Inspection Robot. Procedia Engineering. India, 2014, , 2081 – 2091.
5. Li, H.; Li, R.; Zhang, J.; Zhang, P. Development of a Pipeline Inspection Robot for the Standard Oil Pipeline of China National Petroleum Corporation. Appl. Sci. 2020, 10, 2853.
6. Thomaso, S.; Germano, P.; Martinez, T.; Perriad, Y.. An unethered mechanically-intelligent inchwork robot powered by a shape memory alloy oscillator. Sensors and Actuators A: Physical, 2021; DOI: doi.org/10.1016/j.sna.2021.113115
7. Amakawa T et al 2017 Proposing an adhesion unit for a travelling-wave-type, the omnidirectional wall-climbing robot in airplane body inspection applications 2017 IEEE Int. Conf. on Mechatronics (ICM) (IEEE) 178–83
8. Yum, Y.-J.; Hwang, H.; Kelemen, M.; Maxim, V.; Frankovský, P. In-pipe micromachine locomotion via the inertial stepping principle. J. Mech. Sci. Technol. 2014, 28, 3237–3247.
9. Nieuwenhuisen, M.; Quenzel, J.; Beul, M.; Droeschel, D.; Houben, S.; Behnke, S. (2017). ChimneySpector: Autonomous MAV-based Indoor Chimney Inspection Employing 3D Laser Localization and Textured Surface Reconstruction. 10.1109/ICUAS.2017.7991427.
10. E. Zheng and J. Chen, "A Method for Corrosion Image Acquisition of Chimney Inner," 2019 Chinese Control And Decision Conference (CCDC), 2019, pp. 6411-6415, doi: 10.1109/CCDC.2019.8833044